JOURNAL OF THEORETICAL
AND APPLIED MECHANICS
1, 37, 1999

ABSOLUTE INSTABILITY IN THE COMPRESSIBLE FLOW AROUND A ROTATING CONE

EWA TULISZKA-SZNITKO

Institute of Thermal Engineering, Technical University of Poznań
e-mail: sznitko@sol.put.poznan.pl

In the present paper the character of instability of compressible viscous flow around geometries rotating in the uniform flow is analyzed. The linear local stability theory is used to investigate the boundary layer stability. Following the works of Briggs and Bers in the field of plasma physics, the absolute instability region is identified by the singularities of dispersion relation called pinch-points. The regions of absolute instability in boundary layers of a rotating cone have been found. Calculations have been made for different Mach numbers, wall temperatures and rotational speeds of the cone.

Key words: laminar-turbulent transition, instability

1. Introduction

This paper concerns the space-time evolution of linear instability waves. The flow is excited impulsively at a certain location in space and time. The response of the flow to a impulsive disturbance indicates the type of flow instability i.e., convective or absolute. For the first time the idea of distinction between absolute and convective instability was introduced in the field of plasma physics by Twiss (1951), Briggs (1964) and Bers (1975). The plasma physicists made an extensive contribution to the theoretical development of this idea. The idea was adopted to hydrodynamic instability in spatially evolving shear flows. From the fluid mechanics point of view, it was considered in such survey articles as Brazier-Smith and Scott (1984), Huerre (1987), Monkewitz (1989), Morkovin (1988), Huerre and Monkewitz (1990), and Chomaz et al. (1991).

Following the works of Briggs (1964) and Bers (1975) we define the flow as absolutely unstable if its impulse response grows with time at every location in space. In sufficiently long time a disturbance at a fixed point in space grows to an amplitude which can cause nonlinearity. As a result, in an absolutely unstable flow any infinitesimal disturbance contaminates the entire flow field. If, in contrast, the impulse response decays at every location in sufficiently long time, the flow is convectively unstable. In convectively unstable flow the disturbance is swept away from the source as it grows (Fig.1). The waves travel far enough to reach the amplitude sufficiently large to cause nonlinearity.

In the local linear stability theory we choose either the spatial or temporal theory. In the spatial theory we assume that the wave number is complex and frequency is real so the disturbances grow or decay in space and are periodic in time. In the temporal theory we assume that disturbances grow or decay in time, which implies that frequency is complex and the wave number is real. However, in a real flow disturbances grow or decay in space and time. To find which type of analysis should be used it is necessary to determine the character of instability (absolute or convective). The spatial theory is irrelevant in an absolutely unstable flow.

The reverse mean flow is often cosidered to be related to the absolute instability because it provides a mechanism for upstream effects. The regions of absolutely unstable flows were observed in wake, separation bubbles and on rotating disc in still fluid. The regions of absolute instability for separation bubbles were found by Niew (1993) but the velocity profiles were absolutely unstable only if the region of reverse flow was sufficiently large. Lingwood (1995), (1996), (1997) found the regions of absolute instability in an incompressible boundary layer of disk rotating in still fluid. The laminar velocity profiles for rotating disk boundary layer determined in the directions between the radial and circumferential ones have regions of reverse flow. This model problem is advantegous for there exists an exact similarity solution of the Navier-Stokes equations which is used as a basic state. In the case considered by Lingwood, the flow is fully parallel (the shape of profiles and boundary layer thickness are independent of the radius).

The flow around rotating geometry is often used as a model problem because the boundary layer of rotating geometry is very similar to that of the swept wing flow. Both those boundary layers are strongly three-dimensional and the crossflow instability dominates. Investigations of boundary layers of rotating geometries allow for simpler applications to theory and experiments. Basing on such studies, various hypothesis can be made on a swept wing.

In the present paper we make calculations to find out whether the absolutely unstable flow region exists also in the compressible flow around a cone rotating in a uniform flow. We consider the flow around a sharp cone of zero angle of attack and of a very small half angle Θ (Fig.3). The parallel flow approximation error for the flow around a rotating cone of very small half angle ($\Theta = 0.5° \div 4.0°$) is negligible. This model problem allows us to use the linear local stability theory to analyze the influence of such physical parameters as the edge Mach number and wall temperature in the absolutely unstable region.

2. Absolute instability

In the linear local stability theory the flow is decomposed into a basic state and infinitesimal perturbation. The development of elementary instability waves in the parallel flow is represented by the function

$$f' = \overline{f}(y)e^{i(\alpha x+\beta z-\omega t)} \tag{2.1}$$

where

f'	–	disturbance of an arbitrarily chosen parameter
$\overline{f}$	–	amplitude of disturbance
α, β	–	components of wave number k the streamwise x and spanwise z directions, respectively
ω	–	frequency
y	–	coordinate perpendicular to the wall direction.

In the linear local stability theory the problem of obtaining distributions of the disturbance amplitudes $\overline{f}(y)$ is reduced to solving an eigenvalue problem. The eigenfunctions exist only if k and ω satisfy the following dispersion relation

$$D[k, \omega; \mathrm{Re}] = 0 \tag{2.2}$$

According to the works of Briggs (1964) and Bers (1975) in the field in plasma physics, the flow is absolutely unstable if its impulse response grows with time at every location in space. If the response decays at every location in a sufficiently long time, the flow is convectively unstable. Sketches of the impulse responses in the cases of stable, absolutely unstable and convectively unstable flow are shown in Fig.1a,b,c, respectively.

The impulse excitation gives rise to unstable waves confined within a wedge (Fig.1). The wedge is bounded by two rays of neutral disturbances. In absolutely unstable flows the edges of the wedge move in opposite directions and the point at which the impulse is introduced ($x = 0$, $t = 0$) remains in the unstable region. In convectively unstable flows the edges of the wedge move

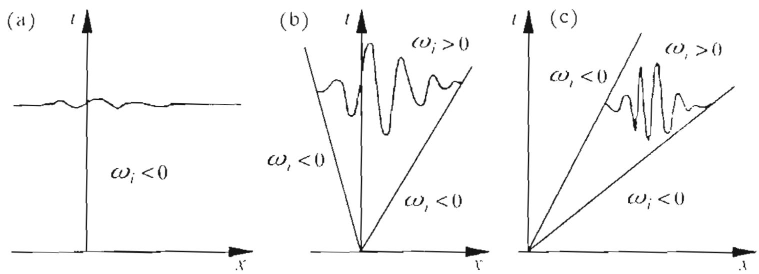

Fig. 1. Sketch of impulse responses: (a) stable flow, (b) absolutely unstable flow. (c) convectively unstable flow (Huerre, 1987)

in the same direction. The point at which the impulse is introduced becomes immediately stable.

The response of a linear system to the forcing input can be determined in terms of the Green function $G(x,t)$. In the physical domain we can write

$$D\Big[-\mathrm{i}\frac{\partial}{\partial x},\mathrm{i}\frac{\partial}{\partial t};\mathrm{Re}\Big]G(x,t)=\delta(x)\delta(t) \tag{2.3}$$

and in the spectral domain

$$D[k,\omega;\mathrm{Re}]G(k,\omega)=1 \tag{2.4}$$

where δ denotes the Dirac function. The flow is absolutely unstable if

$$\lim_{t\to\infty} G(x,t)=\infty \tag{2.5}$$

for every location x and it is convectively unstable if

$$\lim_{t\to\infty} G(x,t)=0 \tag{2.6}$$

Eq (2.3) can be immediately solved in the spectral space

$$G(x,t)=\frac{1}{(2\pi)^2}\int\limits_F\int\limits_L\frac{\mathrm{e}^{\mathrm{i}(kx-\omega t)}}{D[k,\omega;\mathrm{Re}]}\,d\omega dk \tag{2.7}$$

where the path F in the complex plane of wave number k is initially taken as the real axis. The contour L in the complex frequency plane ω is chosen so that the causality holds $G(x,t)=0$ everywhere when $t<0$. The scheme of the contours L and F is shown in Fig.2 (Huerre and Monkewitz, 1990).

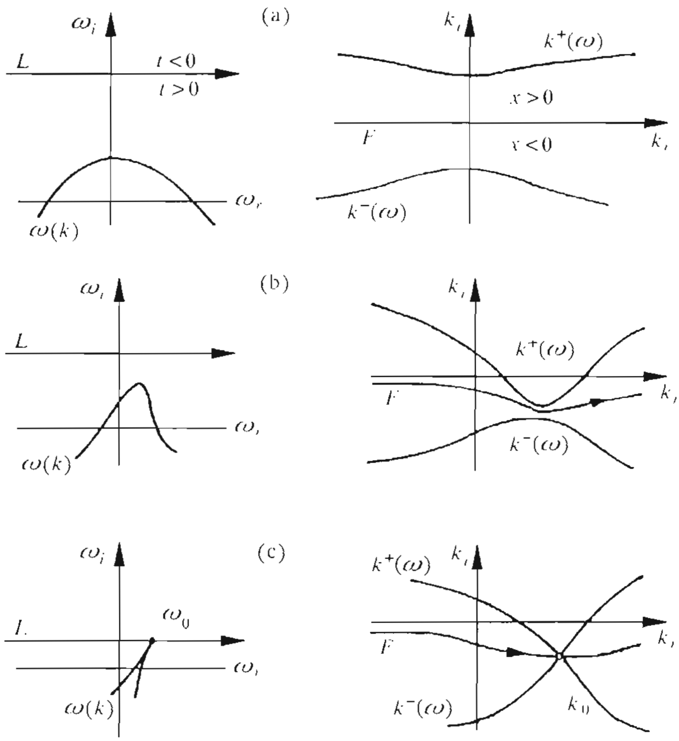

Fig. 2. Different stages of the pinching process. Scheme of spatial $k^+(\omega)$, $k^-(\omega)$ and temporal $\omega(k)$ branches as the L contour is displaced downward in the complex ω plane (Huerre, 1990)

In most cases the Fourier-Laplace integral (2.7) can not be evaluated for arbitrary chosen time; however, for a general dissipation relation one may obtain the time asymptotic Green function. From this asymptotic solution a general mathematical criterion based on the properties of the dispersion relation (2.2) in complex planes k and ω was derived to determine the nature of instability (Briggs, 1964). According to this criterion the absolute instability can be identified by singularities in the dispersion relation called pinch-points. The pinch-points are located in the process of consecutive contour deformations in which L is deformed toward the lower half of ω plane (Kupfer, 1987). The process of deformations of contours of integration is shown schematically in Fig.2.

In Fig.2a the curve $\omega(k)$ is obtained by mapping the F contour along the real k axis into the ω plane by mean of the dispersion relation. If L is located above all singularities of the dispersion relation (above the curve $\omega(k)$

in Fig.2a) its image in the k plane i.e. the spatial branches $k^+(\omega)$, $k^-(\omega)$ must lie in different halves of the k plane (lower and upper half). If one of these spatial branches crosses the original F contour, L itself would intersect the curve $\omega(k)$, which leads to a contradiction. Then, as L is displaced downward, both spatial branches move toward each other (Fig.2b). One of the branches will cross the F contour along the real k axis, so to maintain the causality. the F countour must be deformed off the real k axis to avoid crossing. The process of deformation of F and L contours is finished when F is pinched by the branches $k^+(\omega)$ and $k^-(\omega)$. This point is indicated by k_0 and ω_0. The pinch-points occur precisely at the points where group velocity is zero

$$\frac{\partial\omega}{\partial k}(k_0) = 0 \tag{2.8}$$

We have the following criteria for the absolute instability. The flow is absolutely unstable if the so called absolute amplification rate ω_{0i} is positive ($\omega_{0i} > 0$). Additionally, for the L contour located high enough in the ω plane the spatial branches $k^+(\omega)$ and $k^-(\omega)$ must lie in different halves of k plane.

3. Numerical formulation of the problem

The linear local stability theory of compressible viscous flow is used to investigate the character of instability of strongly three-dimensional boundary layer. The linear local stability equations are derived from the continuity equation, Navier-Stokes equations and energy equation of compressible gas

$$\begin{aligned}
&\frac{\partial\rho}{\partial t} + \nabla\cdot(\rho\boldsymbol{V}) = 0\\
&\rho\Big[\frac{\partial\boldsymbol{V}}{\partial t} + (\boldsymbol{V}\cdot\nabla)\boldsymbol{V}\Big] = -\nabla p - \nabla\times[\mu(\nabla\times\boldsymbol{V})] + \nabla[(\lambda+2\mu)\nabla\cdot\boldsymbol{V}]\\
&\rho c_p\Big[\frac{\partial\tau}{\partial t} + (\boldsymbol{V}\cdot\nabla)\tau\Big] = \nabla\cdot(k\nabla\tau) + \frac{\partial\rho}{\partial t} + (\boldsymbol{V}\cdot\nabla)p + \varPhi
\end{aligned} \tag{3.1}$$

where

$\boldsymbol{V}$ – velocity vector
ρ – density
τ – temperature

μ, λ – first and second viscosity, respectively
c_p – specific heat at constant pressure
t – time
p – pressure
k – coefficient of heat conductivity.

The dissipation function Φ is

$$\Phi = \lambda(\nabla \cdot \boldsymbol{V})^2 + \frac{\mu}{2}(\nabla \boldsymbol{V} + \nabla \boldsymbol{V}^\top)^2 \tag{3.2}$$

In this research we formulate the compressible stability problem in the body-oriented coordinate system (ξ, ζ, η) shown in Fig.3 (ξ, ζ, η are coordinates in the streamwise, wall normal and spanwise directions, respectively). All the lengths are scaled by the viscous scale $LS = \sqrt{\nu_e \xi / U_e}$ and all physical parameters by the corresponding boundary layer edge value. The Reynolds number is defined as follows

$$\mathrm{Re} = \sqrt{\frac{U_e \xi}{\nu_e}} \tag{3.3}$$

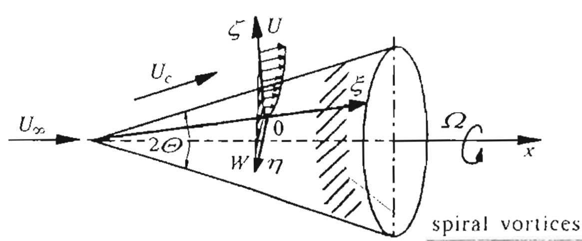

Fig. 3. Scheme of a cone rotating in uniform flow

Perturbation equations are obtained by decomposing all parameters into the steady basic flow $(U, V, W, T, \rho_0, k, \mu_0, \lambda_0)$ and the unsteady disturbance flow components $(u', v', w', \tau', \rho', k', \mu', \lambda')$

$$\begin{array}{lll} u = U + u' & v = V + v' & w = W + w' \\ \tau = T + \tau' & p = P + p' & \rho = \rho_0 + \rho' \\ k = K + k' & \mu = \mu_0 + \mu' & \lambda = \lambda_0 + \lambda' \end{array} \tag{3.4}$$

where u, v, w are velocity components in the ξ, ζ, η directions, respectively.

Substituting Eqs (3.4) into Eqs (3.1) and subtracting from them the equations corresponding to the steady basic state, we obtain the equations for disturbances. Function (2.1) written in the ξ, ζ, η directions describes the development of disturbance in the parallel flow around the cone of zero angle of attack. Linear local stability equations of compressible parallel flow are reduced to the ordinary differential equations

$$(\mathbf{A}D^2 + \mathbf{B}D + \mathbf{C})\boldsymbol{\Psi} = \mathbf{0} \tag{3.5}$$

where $\mathbf{A}$, $\mathbf{B}$, $\mathbf{C}$ are 5×5 matrices and $\boldsymbol{\Psi} = [\overline{u}, \overline{v}, \overline{w}, \overline{\tau}, \overline{p}]^\top$. We have the following homogeneous boundary conditions at the wall and at infinity for the velocity components and temperature amplitude functions

$$\begin{aligned} &\overline{u}(0) = \overline{v}(0) = \overline{w}(0) = \overline{\tau}(0) = 0 \\ &\overline{u}(\zeta) = \overline{v}(\zeta) = \overline{w}(\zeta) = \overline{\tau}(\zeta) = 0 \qquad \zeta \to \infty \end{aligned} \tag{3.6}$$

The linear stability equations (3.5) has been solved using the fourth order accurate two point scheme which has been derived by means of the Euler-Maclaurin formula (Malik, 1982; Balacumar, 1989; Tuliszka-Sznitko, 1993)

$$\varphi^k - \varphi^{k-1} = \frac{h_k}{2}\Big(\frac{d\varphi^k}{d\zeta} + \frac{d\varphi^{k-1}}{d\zeta}\Big) - \frac{h_k^2}{12}\Big(\frac{d^2\varphi^k}{d\zeta^2} - \frac{d^2\varphi^{k-1}}{d\zeta^2}\Big) + 0(h_k^5) \tag{3.7}$$

where $\varphi^k = \varphi(\zeta_k)$, $h_k = \zeta_k - \zeta_{k-1}$.

To apply scheme (3.7) to Eqs (3.5) we formulate them as a set of first order differential equations

$$\frac{d\varphi_n}{d\zeta} = \sum_m^8 a_{nm}\varphi_m \qquad n = 1, ..., 8 \tag{3.8}$$

where

$$\begin{array}{llll} \varphi_1 = \overline{u} & \varphi_2 = d\overline{u}/d\zeta & \varphi_3 = \overline{v} & \varphi_4 = \overline{p} \\ \varphi_5 = \overline{\tau} & \varphi_6 = d\overline{\tau}/d\zeta & \varphi_7 = \overline{w} & \varphi_8 = d\overline{w}/d\zeta \end{array}$$

Final algebraic system of equations with the boundary conditions can be written in the following form

$$\mathbf{A}_k\varphi^{k-1} + \mathbf{B}_k\varphi^k + \mathbf{C}_k\varphi^{k+1} = \mathbf{H}_k \tag{3.9}$$

where $\mathbf{A}_k$, $\mathbf{B}_k$, $\mathbf{C}_k$ are 8×8 matrices and $\mathbf{H}_k$ is 8×1 null matrix. The eigenvalue problem is solved directly. Block elimination method is used to solve algebraic system of equations.

Calculations were made for very small half angle of the cone $\Theta = 0.5° \div 4.0°$ so that the approximation error of the parallel flow mode is negligible. The basic state is obtained from the boundary equations of rotating cone using the Mangler transformations and similarity solutions (Koh and Price, 1967; Illingworth, 1953). The final partial differential equations are solved using the Keller Box method.

4. Results

To find the regions of absolute instability, we apply the Briggs criterion (Briggs, 1964) with a fixed wave number component in the spanwise direction β.

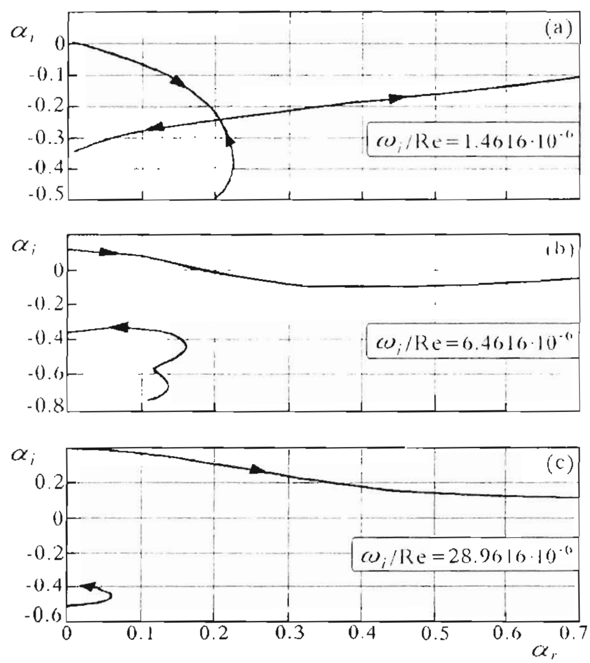

Fig. 4. Development of special branches obtained for different ω_i/Re (Re = 5560, $\mathrm{Ma}_e = 0.21$, $\Theta = 4.0°$, $\Omega/U_e = 19.5$, $\beta = 0.216$, adiabatic wall)

In Fig.4 the development of two spatial branches $\alpha^+(\omega)$, $\alpha^-(\omega)$ in the complex α plane is shown. The results are obtained for the half angle of the cone $\Theta = 4.0°$, edge Mach number $\mathrm{Ma}_e = 0.21$, Reynolds number $\mathrm{Re} = 5560$, rotational speed $\Omega/U_e = 19.5$, component of wave number in spanwise direction $\beta = 0.216$ and for the values of $\omega_i/\mathrm{Re} = 1.4616 \cdot 10^{-6}$ (a), $6.4616 \cdot 10^{-6}$ (b) and $28.9616 \cdot 10^{-6}$ (c). The arrows in Fig.4 indicate the direction of increasing frequency ω_r. In Fig.5 we have a temporal branch $\omega(\alpha)$ obtained for the horizontal line in the α plane $(\alpha_i = -0.24066)$. The tip of this cusp-like form indicates the pinch-point in the ω plane. We have found the pinch-point at $\alpha_0 = (0.20412, -0.24066)$ and $\omega_0/\mathrm{Re} = (134.47 \cdot 10^{-6}, 1.4616 \cdot 10^{-6})$. Absolute amplification rate at this point is positive and

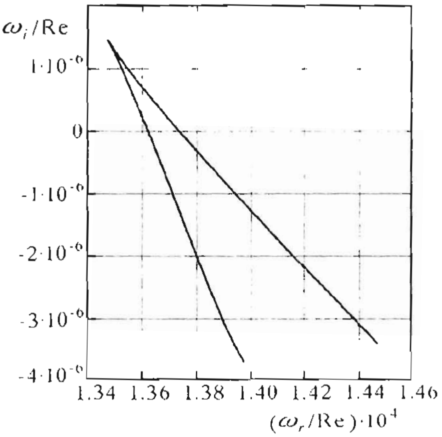

Fig. 5. Result of mapping of the contour $\alpha_i = -0.24066$ from the *alpha* plane to the ω plane (Re $= 5560$, $\mathrm{Ma}_e = 0.21$, $\Theta = 4.0°$, $\Omega/U_e = 19.5$, $\beta = 0.216$, adiabatic wall)

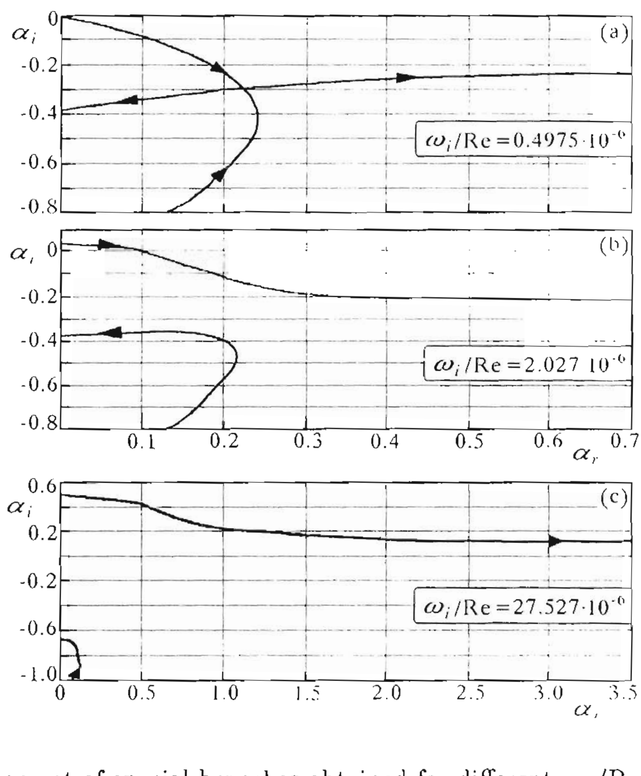

Fig. 6. Development of special branches obtained for different ω_i/Re (Re $= 5760$, $\mathrm{Ma}_e = 0.2$, $\Theta = 0.5°$, $\Omega/U_e = 131.5$, $\beta = 0.316$, adiabatic wall)

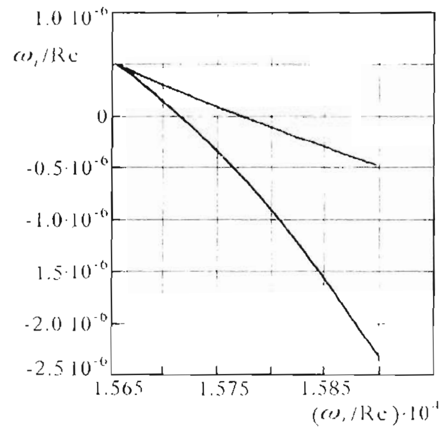

Fig. 7. Results of mapping of the contour $\alpha_i = -0.2945$ from the *alpha* plane to the ω plane ($\mathrm{Re} = 5760$, $\mathrm{Ma}_e = 0.2$, $\Theta = 0.5°$, $\Omega/U_e = 131.5$, $\beta = 0.316$, adiabatic wall)

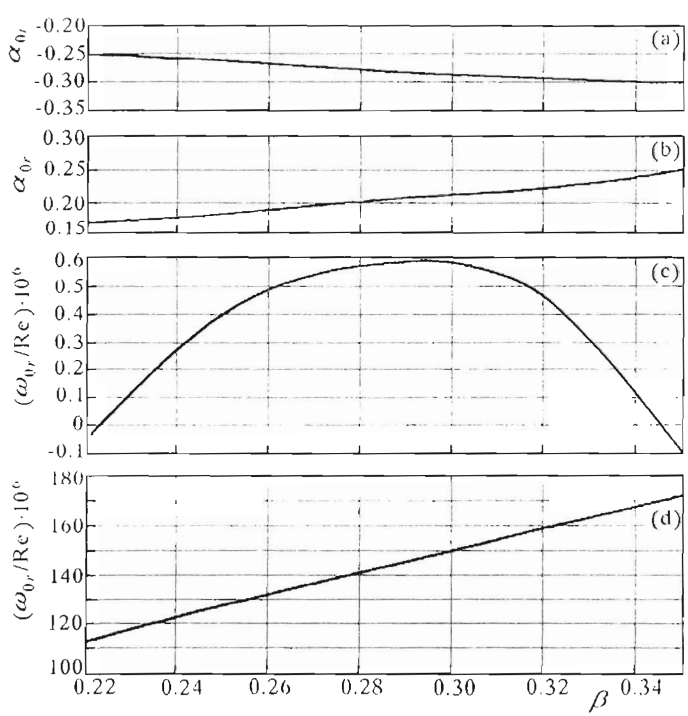

Fig. 8. Variations of α_{0i}, α_{0r}, ω_{0i}/Re and ω_{0i}/Re versus β ($\mathrm{Re} = 5760$, $\mathrm{Ma}_e = 0.2$, $\Theta = 0.5°$, $\Omega/U_e = 131.5$, $\beta = 0.316$, adiabatic wall)

for sufficiently large ω_i the spatial branches $\alpha^+(\omega)$, $\alpha^-(\omega)$ lie in different halves of the α plane so at this point the flow is absolutely unstable.

In Fig.6 and Fig.7 the same analysis is carried out for $\Theta = 0.5°$, $\mathrm{Ma}_e = 0.2$. $\mathrm{Re} = 5760$, $\Omega/U_e = 131.5$, $\beta = 0.316$. Diagrams in Fig.6a,b,c are obtained for $\omega_i/\mathrm{Re} = 0.4975 \cdot 10^{-6}, 2.027 \cdot 10^{-6}, 27.527 \cdot 10^{-6}$, respectively. The pinch-point was found at $\alpha_0 = (0.224, -0.2945)$ and $\omega_0/\mathrm{Re} = (156.56 \cdot 10^{-6}, 0.4975 \cdot 10^{-6})$.

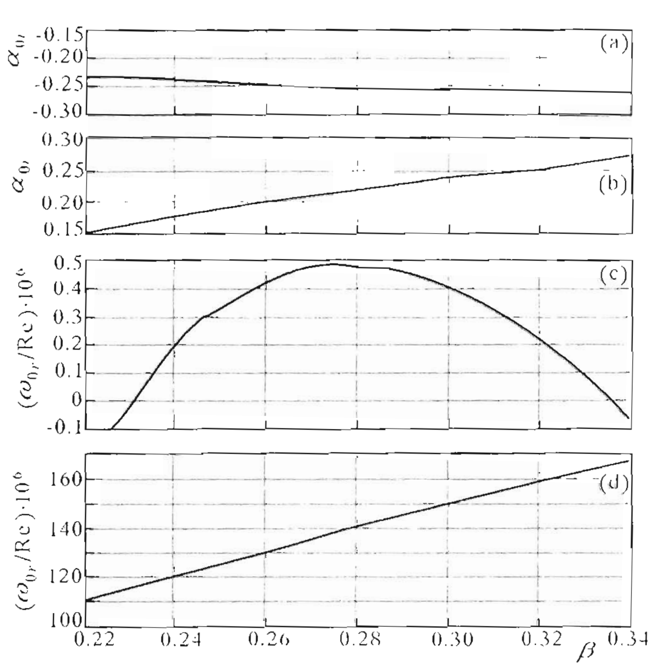

Fig. 9. Variations of α_{0i}, α_{0r}, ω_{0i}/Re and ω_{0i}/Re versus β ($\mathrm{Re} = 5560$, $\mathrm{Ma}_e = 0.2$, $\Theta = 2.0°$, $\Omega/U_e = 31.5$, adiabatic wall)

In Fig.8 and Fig.9 the variations of α_{0i}, α_{0r}, ω_{0i}/Re and ω_{0i}/Re versus β are presented. Calculations were made for different half angles of the cones, different rorational speeds and different Reynolds numbers. The points at which the curves $\omega_{0i}/\mathrm{Re} = f(\beta)$ in Fig.8c and Fig.9c cross the real axis limit the absolutely unstable regions.

Fig.10a,b,c,d show the neutral absolute stability curves obtained in $(\omega_{0r}/\mathrm{Re}, \mathrm{Re})$, $(\alpha_{0i}, \mathrm{Re})$, $(\alpha_{0r}, \mathrm{Re})$ and (β, Re) planes, respectively. Calculations were made for $\Theta = 4.0°$ and $\Omega/U_e = 19.5$. Inside these curves the absolute amplification rates are positive and outside the curves they are negative; consequently, inside of the curves we have the absolutely unstable region and outside the convectively unstable region.

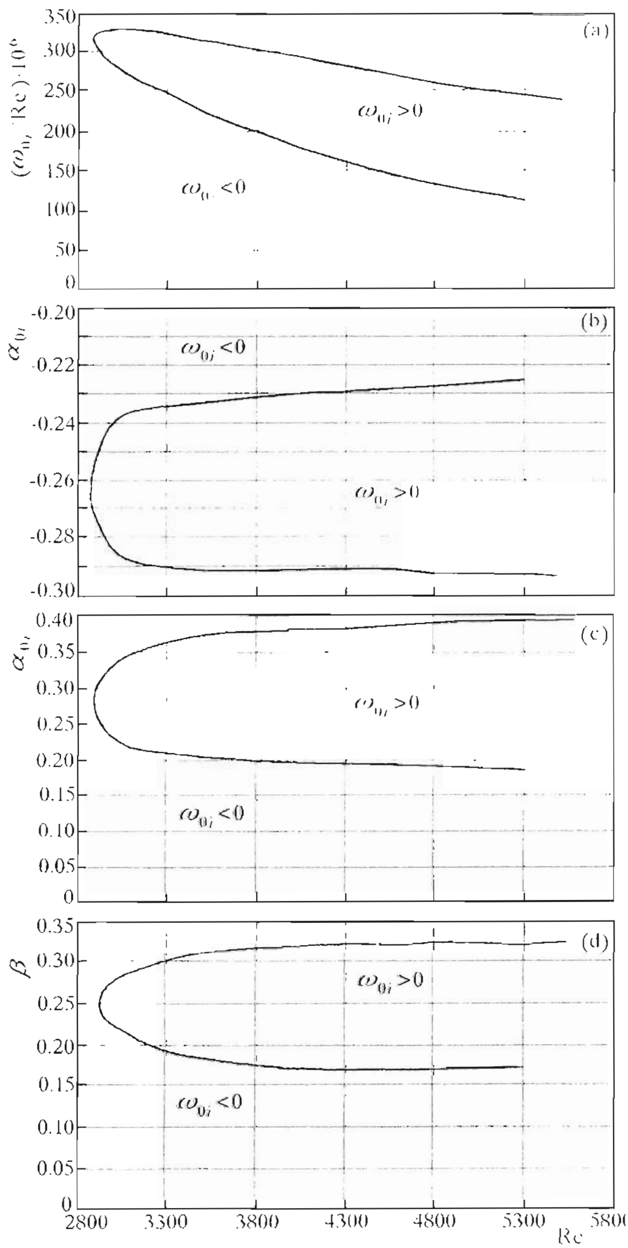

Fig. 10. Absolutely unstable neutral curve ($\mathrm{Ma}_e = 0.21$, $\Theta = 4.0°$ and $\Omega/U_e = 19.5$, adiabatic wall)

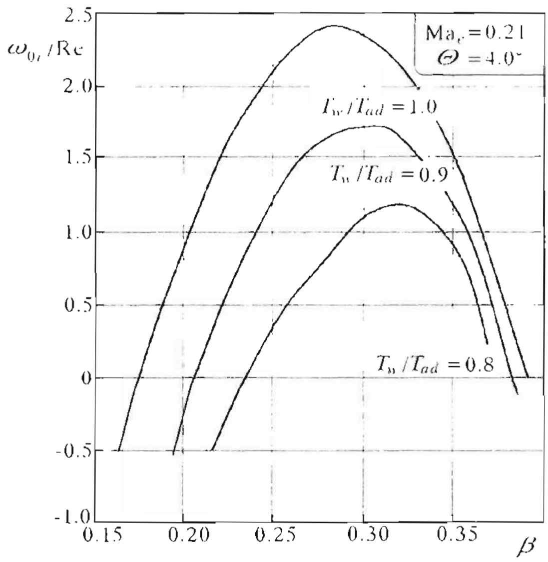

Fig. 11. Variations in the location of pinch-points versus β and temperature rates $T_w/T_{ad} = 1.0$ and 0.8 (Re = 5560, $\Theta = 4.0°$, $Ma_e = 0.21$ and $\Omega/U_e = 19.5$)

The region of absolutely unstable flow decreases with decreasing wall temperature. In Fig.11 the variations of the absolute amplification rate versus β and different temperature rates T_w/T_{ad} are shown (w and ad denote the wall and adiabatic temperatures, respectively). The results are obtained for $\Theta = 4.0°$, $Ma_e = 0.21$, Re = 5560 and $\Omega/U_e = 19.5$. In Fig.12 there are cusp-like forms obtained for the same parameters but for different wall temperatures $T_w/T_{ad} = 1.0$ and 0.8. The absolute amplification rate is smaller for lower wall temperature.

The absolute amplification rates decrease with the increasing edge Mach number. The cusp-like forms obtained for $Ma_e = 0.2$ and $Ma_e = 0.6$ are shown in Fig.13 (Re = 5760, $\Theta = 0.5°$, $\Omega/U_e = 131.5$, $\beta = 0.316$). To obtain positive absolute amplification rates for higher edge Mach numbers it is necessary to increase rotational speed of the cone i. e. it is necessary to increase the crossflow Reynolds number.

In the present paper we also have made calculations to find whether a supersonic flow around a rotating cone can be absolutely unstable. Calculation were made for different (very large) rotational speeds but no pinch-point has been found. The same result for a supersonic flow was obtained by Taylor (1997).

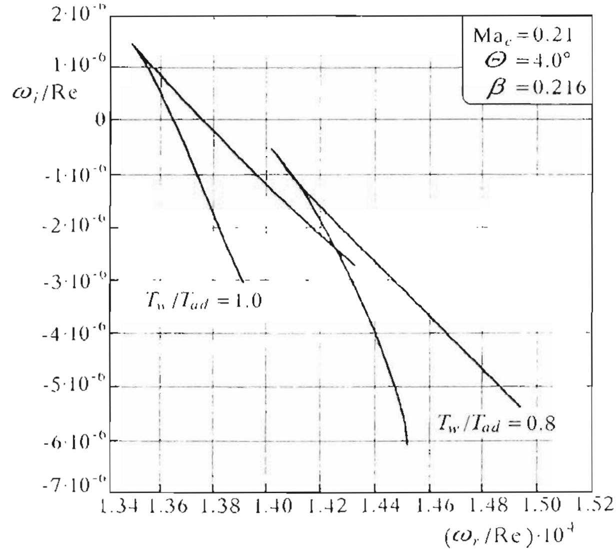

Fig. 12. Cusp-like forms obtained for the wall temperature rates $T_w/T_{ad} = 1.0$ and 0.8 ($Re = 5560$, $\Theta = 4.0°$, $Ma_e = 0.21$, $\Omega/U_e = 19.5$, $\beta = 0.216$)

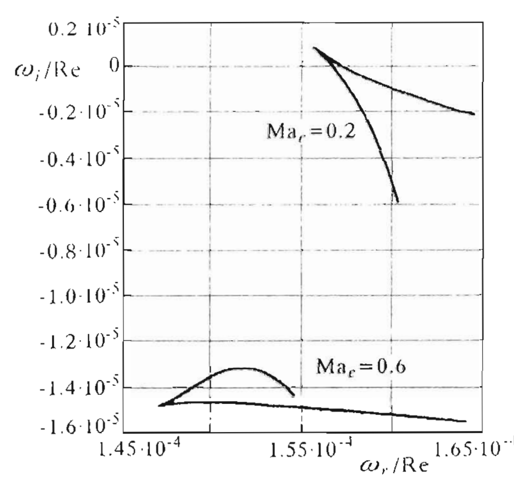

Fig. 13. Cusp-like forms obtained for the Mach number $Ma_e = 0.2$ and 0.6 ($Re = 5760$, $\Theta = 0.5°$, $\Omega/U_e = 131.5$, $\beta = 0.316$, adiabatic wall)

5. Conclusions

In this paper we analyze the character of instability of the flow around a cone of zero angle of attack rotating in a uniform flow. We considered the cone of very small half angle. This model problem allowed us to investigate the influence of such physical parameters as wall temperature and edge Mach number on absolutely unstable flow regions using the linear local stabiliy theory. Convective instability of the flow around a cone rotating in uniform flow was considered in previous works (Tuliszka-Sznitko, 1993, 1996, 1997).

We have found that the boundary layer of cone rotating in the uniform flow can be absolutely unstable over a range of β. We presented the neutral stability curve which showed an absolutely unstable region. We found that the absolute amplification rate decreased with the increasing edge Mach number and decreased with decreasing wall temperature. We did not find absolutely unstable regions in supersonic flows.

The parallel flow approximation can affect the results slightly but the influence of physical parameters on absolutely unstable regions and the general instability characteristics obtained in this paper are still valid.

Acknowledgement

The author is very grateful to Prof. Walter Riess from the University of Hannover for help and cooperation.

References

1. BALACUMAR P., REED H., 1989, Stability of Three Dimensional Boundary Layers, Report of Department of Mechanical and Aerospace Engineering, Arizona State University

2. BERS A., 1975, Linear Waves and Instabilities, in: *Physique des Plasmas* (edit. C. DeWitt, J. Peyraud), Gordon & Breach

3. BRAZIER-SMITH P., SCOTT J., 1984, Stability of Fluid Flow in the Presence of a Compliant Surface, *Wave Motion*, **6**

4. BRIGGS R., 1964, *Electron-Stream Interaction with Plasmas*, MIT Press

5. CHOMAZ J., HUERRE P., REDEKOPP L., 1991, A Frequency Selection Criterion in Spatially Developing Flows, *Stud. Appl. Math.*, **84**

6. HUERE P., 1987, Spatio-Temporal Instabilities in Closed and Open Flows, In: *Instabilities and Nonequilibrium Structures*, edit. E. Tirapegui, D. Villaroel, Dordrecht, Reidel

7. HUERRE P., MONKEWITZ P., 1990, Local and Global Instabilities in Spatially Developing Flows, *Annu. Rev. Fluid. Mech.*, **22**

8. ILLINGWORTH C., 1953, The Laminar Boundary Layer of Rotating Body of Revolution, *Philosophical Magazine*, **44**

9. KOH J., PRICE J., 1967, Nonsimilar Boundary Layer Heat Transfer of a Rotating Cone in Forced Flow, *Transaction of ASME, Journal of Heat Transfer*

10. KUPFER K., BERS A., RAM A., 1987, The Cusp Map in the Complex - Frequency Plane for Absolute Instabilities, *Phys. Fluids*, **30**

11. LINGWOOD R., 1995, Absolute Instability of the Boundary Layer on a Rotating Disk, *J. Fluid. Mech.*, **299**

12. LINGWOOD R., 1996, An Experimental Study of Absolute Instability of the Rotating Disk Boundary Layer Flow, *Fluid. Mech.*, **314**

13. LINGWOOD R., 1997, Absolute Instability of the Ekman Layer and Related Rotating Flows, *J. Fluid. Mech.*, **331**

14. MALIK M., CHUANG S., HUSSAINI M., 1982, Accurate Numerical Solution of Compressible Linear Stability Equations, *ZAMP*, **33**

15. MONKEWITZ P., 1989, The Role of Absolute and Convective Instability in Predicting the Behaviour of Fluid System, *Proc. ASME Fluids Eng. Spring Conf.*, La Jolla, California

16. MORKOVIN M., 1988, Recent Insights into Instability and Transition to Turbulence in Open Flow System, *AIAA Pap.*, 88-3675

17. NIEW T., 1993, The Stability of the Flow in a Laminar Separation Bubble, Ph.D. Thesis, Cambridge University

18. TAYLOR M., 1977, A Causal Stability Analysis of Swept Wing Boundary Layers, *Abstracts of 3rd European Fluid Mechanics Conference*

19. TULISZKA-SZNITKO E., 1993, Niestabilność trójwymiarowej warstwy przyściennej, *WPP Seria Rozprawy*, **287**

20. TULISZKA-SZNITKO E., 1996, Instability of Non-Parallel Compressible Boundary Layer, *MTiS*, **35**, 2

21. TULISZKA-SZNITKO E., 1997, Instability of Boundary Layer on Rotating Geometries, *Numerical Methods in Laminar and Turbulent Flow*, **10**, Pineridge Press, Swansea U.K.

22. TWISS R., 1951, On Oscillations in Electron Stream, *Proc. Phys. Soc. London Sect.*, **B 64**, 654-665

Niestabilność absolutna przepływu ściśliwego wokół wirującego stożka

Streszczenie

W pracy badany jest charakter niestabilności przepływu wokół wirującego stożka. Do badania charakteru przepływu zastosowano kryterium fizyków plazmy Briggsa i Bersa, zgodnie z którym o charakterze niestabilności decydują osobliwości funkcji dyspersji zwane punktami styku. Obliczenia przeprowadzono stosując liniową teorię niestabilności. W pracy stwierdzono występowanie obszarów o niestabilności absolutnej w przepływie wokół wirującego stożka. Obliczenia zostały wykonane dla różnych liczb Macha i różnych temperatur ścianki. Wyznaczono krzywe neutralne ograniczające obszar przepływu o niestabilności absolutnej. Stwierdzono, że współczynnik wzmocnienia absolutnego maleje wraz z rosnącą liczbą Macha, jak również maleje pod wpływem chłodzenia ścianki. Nie stwierdzono występowania niestabilności absolutnej w przepływach naddźwiękowych.

Manuscript received October 2, 1997; accepted for print January 14, 1998